

Eco-evolutionary Spatial Dynamics of Nonlinear Social Dilemmas



Chaitanya S. Gokhale and Hye Jin Park

1 Introduction

The most significant impact of evolutionary game theory has been in the field of social evolution. When an individual's action results in a conflict between the individual and the group benefit, a social dilemma arises. Social dilemmas can be captured by the two-player prisoners dilemma game [6] and its multiplayer version, the public goods game [8, 17, 24]. The domain of public goods games ranges from behavioural economists, cognitive scientists, psychologists, to biologists given the ubiquity of multiplayer interactions in nature. Situations impossible in two-player games can occur in multiplayer games, which can lead to drastically different evolutionary outcomes [7, 14, 35, 39, 44, 52].

In public goods games, while cooperation raises the group benefit, cooperators themselves get less benefit than defectors. The group benefit typically increases linearly with the number of cooperators in the group. However, in the context of helping behaviour, reference [10] discusses a case where each additional cooperator in the group provides more benefit than the previous (superadditivity of benefit). The approach has been further generalised using a particular nonlinear function where the additional cooperators can provide not only more (synergy) but also less (discounting) benefit than the previous cooperator [20]. The study [5] presents an excellent review of the use and importance of nonlinear public goods game.

The nonlinear public goods game as proposed in [20] has been extended in [13] to include population dynamics. In ecological public goods games, the total density of cooperators and defectors changes, effectively changing the interaction group

C. S. Gokhale (✉)

Research Group for Theoretical Models of Eco-evolutionary Dynamics, Department of Evolutionary Theory, Max Planck Institute for Evolutionary Biology, August Thienemann Str-2, 24306 Plön, Germany

e-mail: gokhale@evolbio.mpg.de

H. J. Park

Department of Evolutionary Theory, Max Planck Institute for Evolutionary Biology, August Thienemann Str-2, 24306 Plön, Germany

© The Editor(s) (if applicable) and The Author(s), under exclusive license to Springer Nature Switzerland AG 2020

D. M. Ramsey and J. Renault (eds.), *Advances in Dynamic Games*, Annals of the International Society of Dynamic Games 17, https://doi.org/10.1007/978-3-030-56534-3_8

size. Changes in group size have been shown to result in a stable coexistence of cooperators and defectors [19, 30, 38]. A spatial version of ecological public goods games, where multiple populations of cooperators and defectors are present on a lattice and connected by diffusion, can promote cooperation [53]. The spread of cooperation, in such a case, is possible by a variety of pattern-forming processes.

Their use of spatially extended system in different forms such as grouping, explicit space and deme structures, and other ways of limiting interactions have been studied for long [18, 33, 40, 45, 47, 55]. In particular, in [29], the authors provide conditions for strategy selection in nonlinear games about population structure coefficients. The study cited above by [53] while incorporating ecological dynamics focusses solely on linear public goods games.

Previously we have combined a linear social dilemma with density-dependent diffusion coefficients [12, 37]. Including a dynamic diffusion coefficient comes closer to analysing real movements seen across species from bacteria to humans [16, 23, 27, 28, 32, 34, 43]. Incorporating aspects of ecological games as in [19], spatial dynamics per [53] and nonlinear social dilemmas from [13] we develop our previous approach in this study to nonlinear social dilemmas.

We begin by introducing nonlinearity in the payoff function of the social dilemma, including population dynamics. Then we include simple diffusion dynamics and analyse the resulting spatial patterns. For the parameter set comprising of the diffusion coefficients and the multiplication factor, we can observe the extinction, heterogeneous or homogenous non-extinction patterns. Under certain simplifying assumptions, we can also characterise the stability of the fixed point and discuss the dynamics of the Hopf-bifurcation transition and the phase boundary between heterogeneous- and homogenous-patterned phases. Overall, our results suggest that the spatial patterns while remaining in the same regions relative to each other in the parameter space, synergy and discounting effects shift the boundaries including the phase boundary between extinction and surviving phases. For synergy, the extinction region shrinks as the effective benefit increases resulting in an increased possibility of cooperator persistence. For discounting, however, the extinction region expands. Crucially, the change in the extinction region is not symmetric for synergy and discounting. The above asymmetry is due to the asymmetries in the nonlinear function that we employ for calculating the benefit. The development will help contrast the results with the work of [53] and relates our work to realistic public goods scenarios where the contributions often have a nonlinear impact [9].

2 Model and Results

2.1 *Nonlinear Public Goods Game*

Complexity of evolutionary games increases as we move from two-player games to multiplayer games [14]. A similar trend ensues as we move from linear public

goods games to nonlinear payoff structures [5]. One of the ways of moving from linear to nonlinear multiplayer games is given in [20]. To introduce this method in our notational form, we will first derive the payoffs in a linear setting.

In the classical version of the public goods game (PGG), the cooperators invest c to the common pool while the defectors contribute nothing. The value of the pool increases by a certain multiplication factor r , $1 < r < N$, where N is the group size. The amplified returns are equally distributed to all the N players in the game. For such a setting, the payoffs for cooperators and defectors are given by

$$\begin{aligned} P_D(m) &= \frac{rcm}{N}, \\ P_C(m) &= \frac{rcm}{N} - c, \end{aligned} \quad (1)$$

where m is the number of cooperators in the group. The nonlinearity in the payoffs can be introduced by the parameter Ω as in [20],

$$\begin{aligned} P_D(m) &= \frac{rc}{N}(1 + \Omega + \Omega^2 + \dots + \Omega^{m-1}) = \frac{rc}{N} \frac{1 - \Omega^m}{1 - \Omega}, \\ P_C(m) &= P_D(m) - c = \frac{rc}{N}\Omega(1 + \Omega + \dots + \Omega^{m-2}) + \frac{rc}{N} - c. \end{aligned} \quad (2)$$

If $\Omega > 1$ every additional cooperator contributes more than the previous, thus providing a synergistic effect. If $\Omega < 1$ then every additional cooperator contributes less than the previous, thus saturating the benefits and providing a discounting effect. The linear version of the PGG can be recovered by setting $\Omega = 1$.

As in [19] besides the evolutionary dynamics (change in the frequency of cooperators over time), we are also interested in the ecological dynamics (change in the population density over time). This system analysed in [19, 21] is briefly re-introduced in our notation for later extension. We characterise the densities of cooperators and defectors in the population as u and v . Thus $0 \leq u + v \leq 1$ and the empty space is given by $w = 1 - u - v$. Low population density means that it is hard to encounter other individuals and accordingly hard to interact with them. Hence, the group size N , the maximum group size, in this case, is not always reachable. Instead, S individuals form an interacting group. With fixed N the interacting group size S is bounded, $S \leq N$, and the probability $p(S; N)$ of interacting with $S - 1$ individuals is depending on the total population density $u + v = 1 - w$. When we consider the focal individual, the probability $p(S; N)$ of interacting with $S - 1$ individuals among a maximum group of size $N - 1$ individuals (excluding the focal individual),

$$p(S; N) = \binom{N-1}{S-1} (1-w)^{S-1} w^{N-S}. \quad (3)$$

Then, the average payoffs for defectors and cooperators, f_D and f_C , are given as

$$\begin{aligned} f_D &= \sum_{S=2}^N p(S; N) \overline{P}_D(S), \\ f_C &= \sum_{S=2}^N p(S; N) \overline{P}_C(S), \end{aligned} \quad (4)$$

where $\overline{P}_D(S)$ and $\overline{P}_C(S)$ are the expected payoffs for defectors and cooperators at a given S . The sum for the group sizes S starts at two as for a social dilemma there need to be at least two interacting individuals.

To derive the expected payoffs, we first need to assess the probability of having a certain number of cooperators m in a group of size $S - 1$ which is given by $p_c(m; S)$,

$$p_c(m; S) = \binom{S-1}{m} \left(\frac{u}{1-w} \right)^m \left(\frac{v}{1-w} \right)^{S-1-m}. \quad (5)$$

Thus, the payoffs in Eq. (2) are weighted with the probability of there being m cooperators, giving us the expected payoffs,

$$\begin{aligned} \overline{P}_D(S) &= \sum_{m=0}^{S-1} p_c(m; S) P_D(m), \\ \overline{P}_C(S) &= \sum_{m=0}^{S-1} p_c(m; S) P_C(m+1). \end{aligned} \quad (6)$$

The average payoffs f_D and f_C are thus given by

$$\begin{aligned} f_D &= \frac{r}{N} \frac{1}{1-w-u(1-\Omega)} \left[\frac{(u(\Omega-1)+1)^N - 1}{\Omega-1} - \frac{u(1-w^N)}{1-w} \right], \\ f_C &= f_D - 1 - (r-1)w^{N-1} + \frac{r}{N} \frac{(1-u(1-\Omega))^N - w^N}{1-w-u(1-\Omega)}, \end{aligned} \quad (7)$$

where the investment cost has been set to $c = 1$ without loss of generality. Again, the linear version of the PGG can be recovered by setting $\Omega = 1$,

$$\begin{aligned} f_D &= \frac{ru}{1-w} \left[1 - \frac{(1-w^N)}{N(1-w)} \right], \\ f_C &= f_D - 1 - (r-1)w^{N-1} + \frac{r}{N} \frac{1-w^N}{1-w}. \end{aligned} \quad (8)$$

2.2 Spatial Nonlinear Public Goods Games

For tracing the population dynamics, we are interested in the change in the densities of cooperators and defectors over time. Both cooperators and defectors are assumed to have a baseline birth rate of b and death rate of d . Growth is possible only when

there is empty space available, i.e. $w > 0$. We track the densities of cooperators and defectors by an extension of the replicator dynamics [19, 22, 48],

$$\begin{aligned}\dot{u} &= u[w(f_C + b) - d], \\ \dot{v} &= v[w(f_D + b) - d].\end{aligned}\tag{9}$$

To include spatial dynamics in the above system, we assume that a population of cooperators and defectors resides in a given patch. Game interactions only occur within patches, and the individuals can move adjacent patches. The patches live in a two-dimensional space connected in the form of a regular lattice. Taking a continuum limit, we obtain the differential equations with constant diffusion coefficients for cooperators D_c and defectors D_d ,

$$\begin{aligned}\dot{u} &= D_c \nabla^2 u + u[w(f_C + b) - d], \\ \dot{v} &= D_d \nabla^2 v + v[w(f_D + b) - d].\end{aligned}\tag{10}$$

At the boundaries, there is no in- and out-flux. As in classical activator-inhibitor systems, the different ratio of the diffusion coefficients $D = D_d/D_c$ can generate various patterns from coexistence, extinction as well as chaos [53].

Nonlinearity in PGG is implemented by $\Omega \neq 1$. Previous work shows that the introduction of Ω is enriching the dynamics [13, 20]. Synergy ($\Omega > 1$) enhances cooperation while discounting ($\Omega < 1$) suppresses it. Accordingly, synergy and discounting with a multiplication factor r can map into the linear game with the higher or lower multiplication factor r' , respectively: $r' > r$ for synergy and $r' < r$ for discounting. We call r' as the effective multiplication factor. As shown in Fig. 1, for synergy effect ($\Omega = 1.1$), we can find a chaotic coexistence of cooperators and defectors. The same parameter for a linear case ($\Omega = 1.0$) resulted in total extinction of the population [53]. In the linear case, chaotic patterns were observed for r values larger than that of extinction patterns. Thus, our observation implies the mechanism of how synergy works by effectively increasing r value.

The change in the resulting patterns due to synergy or discounting is not limited to extinction or chaos but is a general feature of the nonlinearity in payoffs. To illustrate this change, we show how a stable pattern under linear PGG ($\Omega = 1$) can change the shape under discounting or synergy in Fig. 2. Such changes in the final structure happen all over the parameter space. To confirm this tendency, we examine the spatial patterns for various parameters and find five phases, same as in the linear PGG case [53] but now with shifted phase boundaries (see Fig. 3). The effective multiplication factor r' increases with an increasing Ω , and thus the location of the Hopf bifurcation also shifts. As a result of shifting r_{Hopf} , extinction region is reduced in the parameter space with synergy effect. We thus focus our attention on the Hopf-bifurcation point r_{Hopf} .

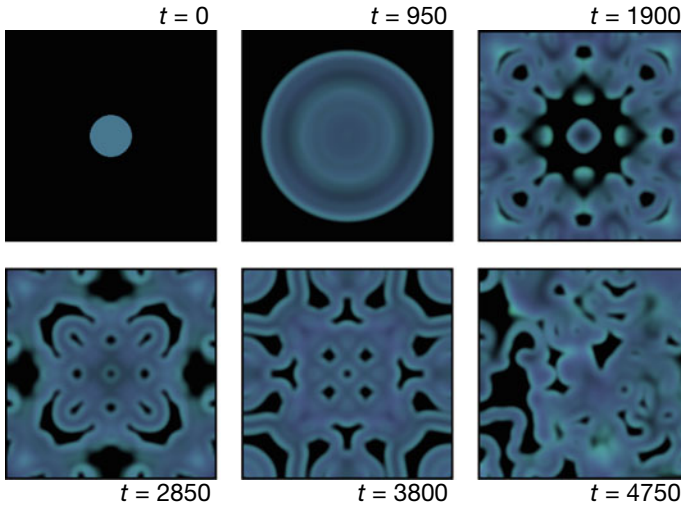


Fig. 1 Pattern formation on the two-dimensional square lattice. We observe the chaotic pattern for $\Omega = 1.1$ (synergy effect) where extinction comes out with $\Omega = 1$ [53]. Mint green and Fuchsia pink colours represent the cooperator and defector densities, respectively. For a full explanation of the colour scheme, we refer to the appendix. Black indicates no individual on the site, whereas blue appears when the ratio of cooperators and defectors is the same. For a system of size L , initially, a disc with radius $L/10$ at the centre is occupied by cooperator and defector with densities 0.1. We use multiplication factor $r = 2.2$ and diffusion coefficient ratio $D = 2$. Throughout the paper, for simulations, we used the system size $L = 283$, $dt = 0.1$ and $dx = 1.4$ with the Crank–Nicolson algorithm

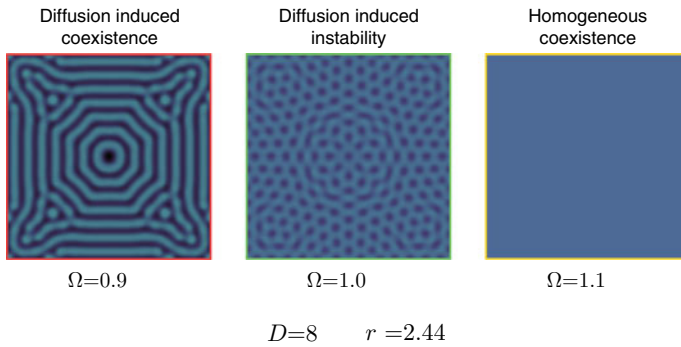


Fig. 2 Synergy and discounting effects on pattern formation. We get the different patterns under discounting and synergy effects distinct from the linear PGG game at a given the same parameter set. While diffusion-induced instability is observed in the linear PGG, the discounting effect makes diffusion-induced coexistence pattern implying that the discounting effect makes the Hopf-bifurcation point shift to the larger value. Under the synergy effect, on the contrary, we obtain the opposite trend observing the homogenous coexistence pattern. In the linear PGG, the homogenous patterns are observed in higher multiplication factor r , implying the shift of r_{Hopf} to the smaller value under the synergy effect

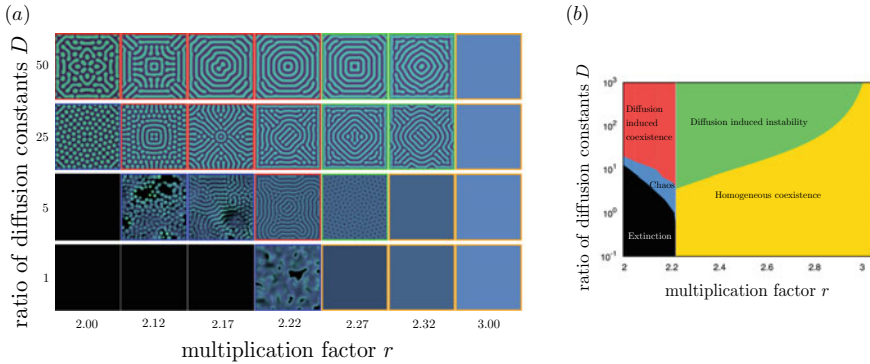


Fig. 3 Spatial patterns and corresponding phase diagram for $\Omega = 1.1$. There are five phases (framed using different colours), extinction (black), chaos (blue), diffusion-induced coexistence (red), diffusion-induced instability (green) and homogeneous coexistence (orange). The Hopf-bifurcation point $r_{\text{Hopf}} \simeq 2.2208$ and the boundary between diffusion-induced instability and homogeneous coexistence are analytically calculated, while the other boundaries are from the simulation results. All boundaries and r_{Hopf} shift to the left, indicating that the multiplication factor r with the synergy maps into the higher multiplication factor r' in the linear game

2.2.1 Hopf Bifurcation in Nonlinear PGG

We find the Hopf-bifurcation point r_{Hopf} for various Ω values using Eq. (7). The effective multiplication factor r' increases as Ω increases, and thus r_{Hopf} is monotonically decreasing with Ω as in Fig. 4a. The tangential line at $\Omega = 1$

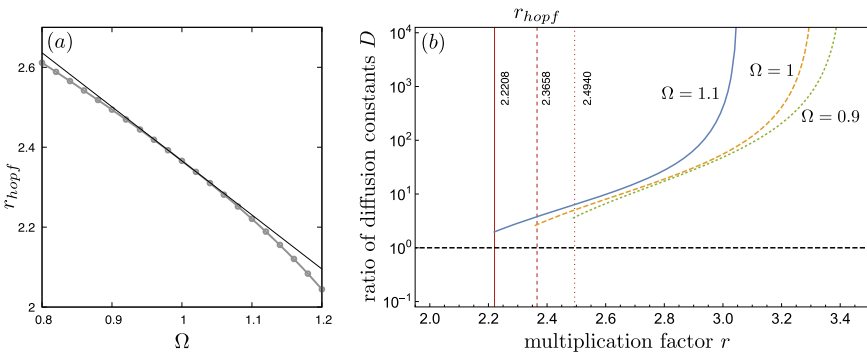


Fig. 4 Hopf-bifurcation points in Ω and shift of the phase boundary. **a** The Hopf-bifurcation point r_{Hopf} for various Ω (solid line with points). Synergy ($\Omega > 1$) decreases r_{Hopf} while discounting ($\Omega < 1$) increases r_{Hopf} . By decreasing r_{Hopf} , the surviving region is extended in the parameter space. The solid line without points is a tangential line at $\Omega = 1$. **b** The phase boundaries between diffusion-induced instability and homogeneous coexistence phases are also examined for various Ω . Since r_{Hopf} increases with a decreasing Ω , the boundaries also move to the right

is drawn for comparing the effects of synergy and discounting. If we focus on the differences between the tangent and r_{Hopf} line, synergy changes r_{Hopf} more dramatically than discounting. Synergy and discounting effects originate from $1 + (1 \pm \Delta\Omega) + (1 \pm \Delta\Omega)^2 + \dots + (1 \pm \Delta\Omega)^{m-1}$ in Eq. (2), where $\Delta\Omega > 0$ and plus and minus signs for synergy and discounting, respectively. Straightforwardly, the difference between 1 and $(1 + \Delta\Omega)^k$ is larger than that of $(1 - \Delta\Omega)^k$ for $k > 2$. Hence, the nonlinear PGG itself gives different Δr_{Hopf} for the same $\Delta\Omega$.

2.2.2 Criterion for Diffusion-Induced Instability

Since Ω changes r' value, the phase boundary also moves. By using the linear stability analysis, we find phase boundaries between diffusion-induced instability and homogeneous coexistence phases in r - D space shown in Fig. 4b. To do that, we introduce new notations, and two reaction–diffusion equations in Eq. (10) can be written as

$$\partial_t \mathbf{u} = \mathbf{D}\nabla^2 \mathbf{u} + \mathbf{R}(\mathbf{u}), \quad (11)$$

with density vector $\mathbf{u} = (u, v)^T$ and matrix $\mathbf{D} = \begin{pmatrix} D_c & 0 \\ 0 & D_d \end{pmatrix}$. Elements of the vector $\mathbf{R}(\mathbf{u}) = \begin{pmatrix} g(u, v) \\ h(u, v) \end{pmatrix}$ indicate reaction terms for each density which is the second terms in Eq. (10). Without diffusion, the differential equations have homogeneous solution $\mathbf{u}_0 = (u_0, v_0)^T$ where $g(u_0, v_0) = h(u_0, v_0) = 0$. We assume that the solution is a fixed point, and examine its stability under diffusion.

If we consider small perturbation $\tilde{\mathbf{u}}$ from the homogeneous solution, $\mathbf{u} \cong \mathbf{u}_0 + \tilde{\mathbf{u}}$, we get the relation,

$$\partial_t \tilde{\mathbf{u}} = \mathbf{D}\nabla^2 \tilde{\mathbf{u}} + \mathbf{J}\tilde{\mathbf{u}}, \quad (12)$$

where $\mathbf{J} = (\partial \mathbf{R} / \partial \mathbf{u})_{\mathbf{u}_0} \equiv \begin{pmatrix} g_u & g_v \\ h_u & h_v \end{pmatrix} \Big|_{\mathbf{u}_0}$. Subscripts of the g and h mean partial derivative of that variable, e.g. g_u means $\partial g / \partial u$. Decomposing $\tilde{\mathbf{u}} = \sum_k \mathbf{a}_k e^{i\mathbf{k}\mathbf{r}}$ based on propagation wave number k gives us relation $\dot{\mathbf{a}}_k = \mathbf{B}\mathbf{a}_k$ where $\mathbf{B} \equiv \mathbf{J} - k^2 \mathbf{D}$. Therefore, the stability of the homogeneous solution can be examined by the matrix \mathbf{B} . Note that $\text{Tr}(\mathbf{B}) < 0$ is guaranteed because $\text{Tr}(\mathbf{J}) < 0$. Hence, if the determinant of \mathbf{B} is smaller than zero [$\det(\mathbf{B}) < 0$], it means one of the eigenvalues of the matrix \mathbf{B} is positive. The homogeneous solution becomes unstable and Turing patterns appear.

The condition for $\det(\mathbf{B}) < 0$ is given by

$$\left(\frac{g_u}{D_c} + \frac{h_v}{D_d} \right)^2 > \frac{4 \det(\mathbf{J})}{D_c D_d}. \quad (13)$$

It can be rewritten as following form:

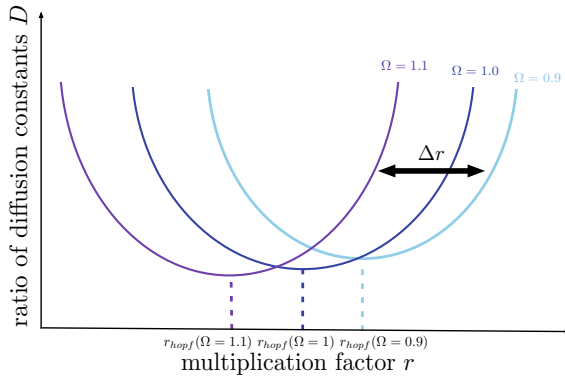


Fig. 5 Schematic figure for expected shift of phase boundaries. According to the change of r_{Hopf} , over all phase boundaries may shift together at the same direction. As we have seen in Fig. 4b, the phase boundaries with r_{Hopf} move to the right with discounting effect and move to the left with synergy effect, respectively. Accordingly, the surviving region in the parameter space expands with synergy effect while it shrinks with discounting effect

$$\frac{D_d}{D_c} > \frac{g_u h_v - 2g_v h_u + 2\sqrt{-g_v h_u \det(\mathbf{J})}}{g_u^2}. \tag{14}$$

With our model parameters this inequality is equivalent to

$$D > \frac{v}{u} \frac{1}{C_u^2} \left[C_u D_v - 2C_v D_u \left(1 - \sqrt{C_v D_u E} \right) \right] \Big|_{u=u^*, v=v^*}, \tag{15}$$

where u^* and v^* are values at the fixed point. The symbols indicate

$$\begin{pmatrix} C_u & C_v \\ D_u & D_v \end{pmatrix} = \begin{pmatrix} d - w^2 \partial_u f_C & d - w^2 \partial_v f_C \\ d - w^2 \partial_u f_D & d - w^2 \partial_v f_D \end{pmatrix}, \tag{16}$$

$$E = C_v \partial_u f_D - C_u \partial_v f_D + d \partial_u f_C - d \partial_v f_C,$$

with $\partial_x y = \frac{\partial y}{\partial x}$. If the above criterion is satisfied, the stable fixed point predicted without diffusion becomes unstable with diffusion (Fig. 5).

3 Discussion

Linear public goods game is a useful approximation of the real nonlinearities in social dilemmas from microbes to macro-life [15, 36, 49] with applications such as in antibiotic resistance [25] as well as cancer [1]. However, taking nonlinearities into account might show different resulting outcomes from naive expectations [13].

Especially, nonlinearities in interactions have a profound effect in ecology when it comes to fecundity and avoiding predation [56, 57]. In this manuscript, we have extended the analysis of spatial public goods games beyond the traditional linear public goods games.

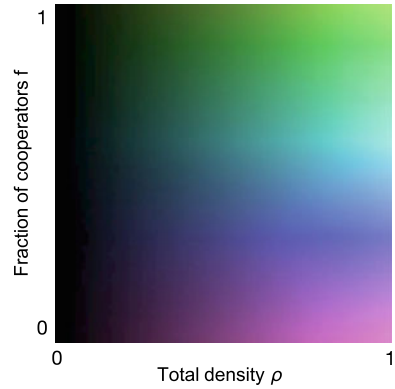
The benefits, in our case, accumulate in a nonlinear fashion in the number of cooperators in the group. Each cooperator can provide a larger benefit than the last one as the number of cooperators increases (resulting in a synergy), or each cooperator provides a smaller benefit than the previous one (thus leading to discounting) [20]. Such an extension to public goods game was proposed very early on by [10]. Termed as superadditivity in benefits, extending from this particular model framework, we can visualise nonlinearities in costs as well, a concept not yet dealt with. Again, such economies of scale [9] can be justified in both bacterial and human interactions as proxies for quorum sensing (or quenching) or accruing of wealth (or austerity) [3, 4, 40].

We show that including such nonlinearities in the benefit function affects the effective rate of return from the public goods game, irrespective of the types of diffusion dynamics. With spatial dynamics, synergy increases the effective rate of return on the investment and expands the region in the parameter space where survival of the population is possible. This itself may make cooperation a favourable strategy. Besides the trivial observation that synergy helps cooperators, we show that as we move symmetrically away from the linear case towards more synergy or discounting, the change in the eventual dynamics is not symmetric. It would be interesting to check if the asymmetry holds for different designs of benefit functions.

We used the particular functional form of the benefit function, including nonlinearities in payoffs [20]. However, there are various ways of including nonlinearities in the benefit function [4, 7, 40]. The model considered in [40] extends the results of [20] to games between relatives. Furthermore, [40] has described the relationships between different nonlinear social dilemma models with a variety of benefit functions. Also these nonlinear social dilemmas have been analysed in a structured population [29, 40, 41]. However, previous studies have focused on the approach presented in [46], which provide a criterion for strategy selection rather than explicitly positioning the populations on a grid and including diffusion. When studying games in structured populations, often a network structure is considered [2, 42]. The role of network connectivity is determined to be critical for the eventual evolutionary outcome [41, 50, 51] and some structures can result in hindering the evolution of cooperation as well [26]. In contrast, our approach focuses more on the ecological framework but not in network structures. We take into account not only the changes in frequencies of cooperators and defectors but also the population dynamics, which is usually missed in a network approach. While both approaches make evolutionary games ecologically explicit, the models are thoroughly different in their setup and implementation.

The importance of including ecology in evolutionary games has been known for long, but the complexity that it generates has prevented it from garnering widespread attention [11]. Seasonal variations in the rate of return radically change the selection pressures on cooperation and defection. Changes in the ecology may not feedback

Fig. 6 The exact colour scheme developed for colouring the patterns. Each patch in a pattern is coloured using this palette by choosing the corresponding f and ρ values. For brightness we used Eq. (17) with $a = 15$



directly to the frequencies of cooperators and defectors but on to a variable in benefit–cost functions. If the variable affects the frequency of cooperators and defectors (or even the group size) in a nonlinear fashion, then the results are not trivial [13, 38]. Thus, even a simple connection between evolutionary and ecological dynamics may already generate rich dynamics [31, 54], and the feedback between the two is often already convoluted. Similar to [12, 37], it is possible to include feedback between the population dynamics and diffusion here, but together with a nonlinear social dilemma, we envision that the formal analysis and the computational implementation will be a considerable challenge.

Acknowledgments We thank Christoph Hauert for comments and suggestions in improving an early version of the manuscript. The authors thank the constructive comments of the reviewers. Both authors acknowledge generous support from the Max Planck Society.

Appendix

Colour Coding

Similar to the colour coding used in [37] we use mint green (colour code: #A7FF70) and Fuchsia pink (colour code: #FF8AF3) colours for denoting the cooperator and defector densities, respectively, for each type. The colour spectrum and saturation is determined by the ratio of cooperators to defectors which results in the Maya blue colour for equal densities of cooperators and defectors. For convenience, we use HSB colour space which is a cylindrical coordinate system $(r, \theta, h) = (\text{saturation, hue, brightness})$. The radius of circle r indicates saturation or the colour whereas θ helps us transform the RGB space to HSB. The total density of the population $\rho = u + v$ is represented by the brightness h of the colour. For better visualisation, we formulate the brightness h as

$$\frac{\log a\rho + 1}{\log a + 1}, \quad (17)$$

where a control parameter a (> -1 and $\neq 0$) (see Fig. 6). The complete colour scheme so developed passes the standard tests for colour blindness.

References

1. Aktipis A (2016) Principles of cooperation across systems: from human sharing to multicellularity and cancer. *Evolutionary Applications* 9(1):17–36
2. Allen B, Lipper G, Chen YT, Fotouhi B, Nowak MA, Yau ST (2017) Evolutionary dynamics on any population structure. *Nature* 544:227–230
3. Archetti M (2009) Cooperation as a volunteer's dilemma and the strategy of conflict in public goods games. *Journal of Evolutionary Biology* 11:2192–2200
4. Archetti M, Scheuring I (2011) Co-existence of cooperation and defection in public goods games. *Evolution* 65(4):1140–1148
5. Archetti M, Scheuring I (2012) Review: Game theory of public goods in one-shot social dilemmas without assortment. *Journal of Theoretical Biology* 299(0):9–20
6. Axelrod R (1984) *The evolution of cooperation*. Basic Books, New York, NY
7. Bach LA, Helvik T, Christiansen FB (2006) The evolution of n -player cooperation - threshold games and ESS bifurcations. *Journal of Theoretical Biology* 238:426–434
8. Binmore KG (1994) *Playing fair: game theory and the social contract*. MIT Press, Cambridge
9. Dawes RM, Orbell JM, Simmons RT, Van De Kragt AJC (1986) Organizing groups for collective action. *The American Political Science Review* 80(4):1171–1185
10. Eshel I, Motro U (1988) The Three Brothers' Problem: Kin Selection with More than One Potential Helper. 1. The Case of Immediate Help. *The American Naturalist* 132(4):550–566
11. Estrela S, Libby E, Van Cleve J, Débarre F, Deforet M, Harcombe WR, Peña J, Brown SP, Hochberg ME (2018) Environmentally Mediated Social Dilemmas. *Trends in Ecology & Evolution* 34(1):6–18
12. Funk F, Hauert C (2019) Directed migration shapes cooperation in spatial ecological public goods games. *PLOS Computational Biology* 15(8):1–14
13. Gokhale CS, Hauert C (2016) Eco-evolutionary dynamics of social dilemmas. *Theoretical Population Biology* 111:28–42
14. Gokhale CS, Traulsen A (2010) Evolutionary games in the multiverse. *Proceedings of the National Academy of Sciences USA* 107:5500–5504
15. Gore J, Youk H, van Oudenaarden A (2009) Snowdrift game dynamics and facultative cheating in yeast. *Nature* 459:253–256
16. Grauwin S, Bertin E, Lemoy R, Jensen P (2009) Competition between collective and individual dynamics. *Proceedings of the National Academy of Sciences of the United States of America* 106(49):20,622–20,626
17. Hardin G (1968) The tragedy of the commons. *Science* 162:1243–1248
18. Hauert C, Imhof L (2012) Evolutionary games in deme structured, finite populations. *Journal of Theoretical Biology* 299:106–112
19. Hauert C, Holmes M, Doebeli M (2006a) Evolutionary games and population dynamics: maintenance of cooperation in public goods games. *Proceedings of the Royal Society B* 273:2565–2570
20. Hauert C, Michor F, Nowak MA, Doebeli M (2006b) Synergy and discounting of cooperation in social dilemmas. *Journal of Theoretical Biology* 239:195–202
21. Hauert C, Yuichiro Wakano J, Doebeli M (2008) Ecological public goods games: cooperation and bifurcation. *Theoretical Population Biology* 73:257–263

22. Hofbauer J, Sigmund K (1998) *Evolutionary Games and Population Dynamics*. Cambridge University Press, Cambridge, UK
23. Kawasaki K, Mochizuki A, Matsushita M, Umeda T, Shigesada N (1997) Modeling spatio-temporal patterns generated by *Bacillus subtilis*. *Journal of Theoretical Biology* 188:177–185
24. Kollock P (1998) Social dilemmas: The anatomy of cooperation. *Annual Review of Sociology* 24:183–214
25. Lee HH, Molla MN, Cantor CR, Collins JJ (2010) Bacterial charity work leads to population-wide resistance. *Nature* 467(7311):82–85
26. Li A, Broom M, Du J, Wang L (2016) Evolutionary dynamics of general group interactions in structured populations. *Physical Review E* 93(2):022,407
27. Loe LE, Mysterud A, Veiberg V, Langvatn R (2009) Negative density-dependent emigration of males in an increasing red deer population. *Proc R Soc B* 276:2581–2587
28. Lou Y, Martínez S (2009) Evolution of cross-diffusion and self-diffusion. *Journal of Biological Dynamics* 3(4):410–429
29. McAvoy A, Hauert C (2016) Structure coefficients and strategy selection in multiplayer games. *Journal of Mathematical Biology* pp 1–36
30. McAvoy A, Fraiman N, Hauert C, Wakeley J, Nowak MA (2018) Public goods games in populations with fluctuating size. *Theoretical Population Biology* 121:72–84, <https://doi.org/10.1016/j.tpb.2018.01.004>
31. McNamara JM (2013) Towards a richer evolutionary game theory. *Journal of The Royal Society Interface* 10:20130,544
32. Ohgiwari M, Matsushita M, Matsuyama T (1992) Morphological changes in growth phenomena of bacterial colony patterns. *J Phys Soc Jap* 61:816–822
33. Ohtsuki H, Pacheco J, Nowak MA (2007) Evolutionary graph theory: Breaking the symmetry between interaction and replacement. *Journal of Theoretical Biology* 246:681–694
34. Okubo A, Levin SA (1980) *Diffusion and Ecological Problems: Mathematical Models*. Springer-Verlag
35. Pacheco JM, Santos FC, Souza MO, Skyrms B (2009) Evolutionary dynamics of collective action in n-person stag hunt dilemmas. *Proceedings of the Royal Society B* 276:315–321
36. Packer C, Rutten L (1988) The evolution of cooperative hunting. *The American Naturalist* 132:159–198
37. Park HJ, Gokhale CS (2019) Ecological feedback on diffusion dynamics. *Journal of the Royal Society Open Science* 6:181,273
38. Peña J (2012) Group size diversity in public goods games. *Evolution* 66:623–636
39. Peña J, Lehmann L, Nöldeke G (2014) Gains from switching and evolutionary stability in multi-player matrix games. *Journal of Theoretical Biology* 346:23–33
40. Peña J, Nöldeke G, Lehmann L (2015) Evolutionary dynamics of collective action in spatially structured populations. *Journal of Theoretical Biology* 382:122–136
41. Peña J, Wu B, Arranz J, Traulsen A (2016) Evolutionary games of multiplayer cooperation on graphs. *PLoS Computational Biology* 12(8):1–15
42. Santos FC, Pacheco JM, Lenaerts T (2006) Evolutionary dynamics of social dilemmas in structured heterogeneous populations. *Proceedings of the National Academy of Sciences USA* 103:3490–3494
43. Shigesada N, Kawasaki K, Teramoto E (1979) Spatial segregation of interacting species. *Journal of Theoretical Biology* 79(1):83–99
44. Souza MO, Pacheco JM, Santos FC (2009) Evolution of cooperation under n-person snowdrift games. *Journal of Theoretical Biology* 260:581–588
45. Tarnita CE, Antal T, Ohtsuki H, Nowak MA (2009a) Evolutionary dynamics in set structured populations. *Proceedings of the National Academy of Sciences USA* 106:8601–8604
46. Tarnita CE, Ohtsuki H, Antal T, Fu F, Nowak MA (2009b) Strategy selection in structured populations. *Journal of Theoretical Biology* 259:570–581
47. Tarnita CE, Wage N, Nowak MA (2011) Multiple strategies in structured populations. *Proceedings of the National Academy of Sciences USA* 108:2334–2337

48. Taylor PD, Jonker LB (1978) Evolutionarily stable strategies and game dynamics. *Mathematical Biosciences* 40:145–156
49. Turner PE, Chao L (1999) Prisoner's Dilemma in an RNA virus. *Nature* 398:441–443
50. van Veelen M, Nowak MA (2012) Multi-player games on the cycle. *Journal of Theoretical Biology* 292:116–128
51. van Veelen M, García J, Rand DG, Nowak MA (2012) Direct reciprocity in structured populations. *Proceedings of the National Academy of Sciences USA* 109:9929–9934
52. Venkateswaran VR, Gokhale CS (2019) Evolutionary dynamics of complex multiple games. *Proceedings of the Royal Society B: Biological Sciences* 286(1905):20190,900
53. Wakano JY, Nowak MA, Hauert C (2009) Spatial dynamics of ecological public goods. *Proceedings of the National Academy of Sciences USA* 106:7910–7914
54. Weitz JS, Eksin C, Paarporn K, Brown SP, Ratcliff WC (2016) An oscillating tragedy of the commons in replicator dynamics with game-environment feedback. *Proceedings of the National Academy of Sciences of the United States of America* 113(47):E7518–E7525
55. Wright S (1930) The genetical theory of natural selection. *Journal of Heredity* 21:349–356
56. Wrona FJ, Jamieson Dixon RW (1991) Group Size and Predation Risk: A Field Analysis of Encounter and Dilution Effects. *The American Naturalist* 137(2):186–201
57. Zöttl M, Frommen JG, Taborsky M (2013) Group size adjustment to ecological demand in a cooperative breeder. *Proceedings of the Royal Society B: Biological Sciences* 280(1756):20122,772